Experimental investigation of concrete-filled and bare 6082-T6 aluminium alloy tubes under in-plane bending

Shafayat Bin Ali, George S. Kamaris, Michaela Gkantou, Kunal D. Kansara
School of Civil Engineering and Built Environment, Liverpool John Moores University, Liverpool, United Kingdom.
S.B.Ali@2019.ljmu.ac.uk, G.Kamaris@ljmu.ac.uk, M.Gkantou@ljmu.ac.uk, K.D.Kansara@ljmu.ac.uk

ABSTRACT

The application of aluminium alloys in construction sector is increasing owing to their excellent corrosion resistance, light weight and attractive appearance. However, one of the main disadvantages of aluminium alloys is the low elastic modulus, which may cause a stability issue in aluminium structural members. The performance of aluminium tubes can be improved by filling concrete within them. Research on the flexural behaviour of concrete-filled aluminium alloy tubes is limited. This paper presents an experimental study on the behaviour of square and rectangular concrete-filled and bare aluminium tubular sections subjected to in-plane bending. Total 20 beams were tested, including 10 concrete-filled aluminium tubes (CFAT) and 10 bare aluminium tubes (BAT). The hollow aluminium tubes were fabricated using 6082-T6 alloy and filled with 25 MPa cylinder compressive strength concrete. The material properties of aluminium were measured by tensile test of coupons. It is shown that the flexural strength, stiffness and ductility of square and rectangular BAT flexural members was remarkably improved by the infilled concrete and the improvement is more pronounced for the thinner aluminium sections. Due to absence of design standards for CFAT beams, in this study the design rules available for concrete-filled steel tubular flexural members in the Eurocode 4 are considered by substituting the mechanical properties of steel with those of aluminium alloy. It is demonstrated that the proposed design rules provide good predictions of the flexural capacity of CFAT.

KEYWORDS: *6082-T6 Aluminium alloy, Concrete-filled sections, Bare sections, Four-point bending, Flexural behaviour.*

1 INTRODUCTION

The application of aluminium alloys in construction sector is increasing owing to their superior properties including excellent corrosion resistance, light weight, ease of production, high recyclability and attractive appearance (Mazzolani, 2004; Georgantzia, Gkantou, & Kamaris, 2021). However, one of the main disadvantages of aluminium alloys is the low elastic modulus, which may cause a stability issue of aluminium structural members (Mazzolani, 1995; Zhu & Young, 2008). Hence, concrete-filled aluminium alloy tubular (CFAT) structural members are introduced to improve the performance of bare aluminium alloy tubular (BAT) ones. Concrete-filled steel tubular (CFST) structural members are increasingly applied in modern construction because of their several advantages such as, high bearing capacity, ductility, fire resistance etc. The weight of the CFST members can be reduced significantly by replacing the steel tube with aluminium tube (Patel, Liang & Hadi 2020).

A considerable number of research was performed to study the flexural response of CFST beams. Lu and Kennedy (1994) conducted an experimental investigation on the behaviour of CFST beams and demonstrated that the flexural strength of CFST members significantly increased due to the concrete infill. Han (2004) carried out research on structural response of CFST beams and suggested a method to determine the flexural capacity of CFST members. Montuori and Piluso (2015) performed tests on CFST beams under non-uniform bending and suggested a fibre model to predict the bending strength of CFST members. A test programme was conducted by Hou et al (2016) to investigate the influence of chloride corrosion on the flexural behaviour of CFST beams. They found that the chloride corrosion noticeably

ISSN 2961-5011 | https://doi.org/10.54389/ZXCY2044

affected the bending capacity and ductility of the members. Chen et al (2017a, 2017b) experimentally determined the bending stiffness of concrete-filled stainless-steel tubular beams and compared it with the design stiffness calculated using the British, European, American and Japanese standards. They showed that the existing design standards are conservative in calculating the design stiffness of CFST sections made with stainless steel. Zhang et al (2021) investigated the flexural response of elliptical CFST beams and suggested equations to calculate the bending strength and stiffness of the members.

Numerous research studies were conducted to investigate the flexural behaviour of BAT flexural members. Moen et al (1999a, 1999b) studied the flexural strength and rotational capacity of 6082 and 7108 aluminium alloy beams with welded stiffeners. They demonstrated that due to welding the aluminium alloy flexural members experienced premature tensile failure, which resulted in reduction of rotation capacity. Zhu and Young (2009) investigated the behaviour of 6061-T6 aluminium alloy beams under in-plane bending and suggested design equations to predict design capacity. Su, Young and Gardner (2014) conducted research on the bending response of 6061-T6 and 6063-T5 aluminium alloy hollow sections. They compared the experimental flexural strength with the design strength determined by the European, American and Australian standards and concluded that the design specifications are conservative. Feng et al (2017) studied the structural response of perforated BAT beams made with 6061-T6 and 6063-T5 grade alloys and demonstrated that the North American specifications are appropriate for designing perforated aluminium alloy beams.

Previous research has focused on the behaviour of CFST beams, whereas research on the structural behaviour of CFAT flexural members is limited. Moreover, minimal number of research studies exist on the flexural response of BAT beams made with 6082-T6 alloy. Nowadays, the 6082 grade aluminium alloy has gained more popularity in modern construction (Kissell and Ferry, 2002) because of its high bearing capacity, corrosion resistance and weldability. This paper presents an experimental study on the performance of CFAT and BAT beams subjected to in-plane bending. The square and rectangular hollow aluminium sections were made of 6082-T6 alloy. The structural response of the specimens is presented by failure mode, flexural strength, flexural stiffness, and ductility. Due to absence of design standards for CFAT beams, in this study the design equations available for concrete-filled steel tubular flexural members in Eurocode 4 (2004) are considered by substituting the mechanical properties of steel with those of aluminium alloy.

2 EXPERIMENTAL INVESTIGATION

2.1 Test Specimens

Total 20 square and rectangular beams were tested subjected to in-plane bending, whereas 10 were concrete filled and 10 were bare specimens. The aluminium tubes were fabricated by 6082-T6 alloy. The specimens' length was 1000 mm. The dimensions of all specimens measured before the tests are presented in Table 1. The label of a specimens was given based on its cross-sectional measurements. For example, the label '101.6×25.4×3.3-C' refers to a specimen with depth (D) of 101.6 mm, width (B) of 25.4 mm and thickness (t) of 3.3 mm and the notation '-C' refers to the existence of concrete infill. Figure 1 presents the geometric properties of typical BAT and CFAT sections.

For CFAT specimen, a wooden plate was attached by tape at the bottom end of each hollow tube to avoid any leakage of concrete. During casting, the concrete was filled in layers and compacted by a vibrating table. All specimens were enclosed by plastic sheet and kept 28 days for self-curing.

Table 1. Measured cross-sectional dimensions of all specimens.

Specimen	*D* (mm)	*B* (mm)	*t* (mm)	Specimen	*D* (mm)	*B* (mm)	*t* (mm)
76.2×76.2×1.6	76.3	76.2	1.54	76.2×76.2×1.6-C	76.3	76.2	1.54
76.2×76.2×3.3	76.2	76.2	3.21	76.2×76.2×3.3-C	76.2	76.2	3.21
76.2×76.2×4.8	76.2	76.1	4.71	76.2×76.2×4.8-C	76.2	76.1	4.71
76.2×76.2×6.4	76.2	76.2	6.21	76.2×76.2×6.4-C	76.2	76.2	6.21
76.2×25.4×3.3	76.3	25.5	3.33	76.2×25.4×3.3-C	76.3	25.5	3.32
76.2×38.1×3.3	76.2	38.3	3.26	76.2×38.1×3.3-C	76.2	38.3	3.26
76.2×50.8×3.3	76.1	50.7	3.15	76.2×50.8×3.3-C	76.1	50.7	3.15
101.6×25.4×3.3	101.6	25.4	3.21	101.6×25.4×3.3-C	101.6	25.4	3.20
101.6×50.8×3.3	101.9	51.4	3.44	101.6×50.8×3.3-C	101.9	51.4	3.41
101.6×76.2×3.3	101.5	76.3	3.14	101.6×76.2×3.3-C	101.5	76.3	3.14

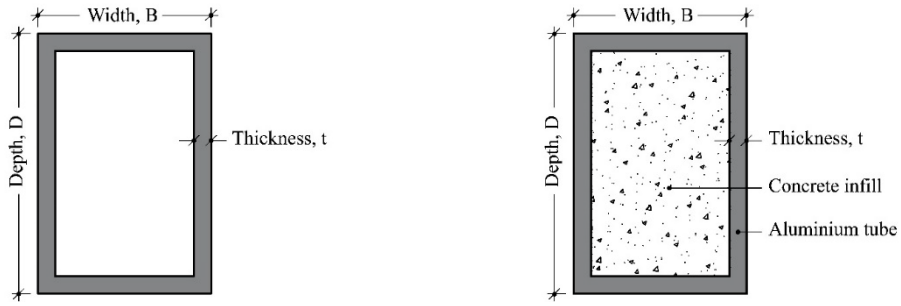

(a) (b)

Figure 1. Cross-sections of a typical (a) BAT beam, (b) CFAT beam.

2.2 Material properties

The mechanical properties of aluminium alloy sections were determined by tensile test of coupons. The coupons with gauge length and width of 100 mm and 12 mm, respectively were collected from each specimen based on the recommendation of BS EN ISO 6892-1 (2009). The tests were conducted using a 50 kN capacity machine and displacement-control load of 0.2 mm/min was applied during the tests. The longitudinal strains of the coupons were measured by an extensometer. The mechanical properties found from the coupon tests are listed in Table 2, where *E* debote modulus of elasticity, $\sigma_{0.1}$ is 0.1% proof stress, $\sigma_{0.2}$ is 0.2% proof stress, σ_u is ultimate stress, ε_u is the ultimate strain and ε_f is the strain at rupture.

Table 2. Mechanical properties of aluminium alloy tubes.

Specimen	*E* (GPa)	$\sigma_{0.1}$ (MPa)	$\sigma_{0.2}$ (MPa)	σ_u (MPa)	ε_u (%) (mm/mm)	ε_f (%) (mm/mm)
76.2×76.2×1.6	67.9	288.4	292.9	316	6.9	8.4
76.2×76.2×3.3	66.2	295.2	299.1	321	7.5	10.5
76.2×76.2×4.8	64.7	303.7	306.1	316	6.3	9.7
76.2×76.2×6.4	69.3	290.4	295.3	326	8.8	15.3
76.2×25.4×3.3	68.9	271.8	277.9	316	8.8	14.3
76.2×38.1×3.3	68.5	270.4	276.8	315	7.8	9.3
76.2×50.8×3.3	67.5	285.9	289.5	312	7.1	9.1
101.6×25.4×3.3	63.9	234.7	242.5	290	7.6	13.2
101.6×50.8×3.3	71.6	166.9	175.1	204	7.4	12.1
101.6×76.2×3.3	72.8	303.5	306.7	320	5.6	6.9

For concrete mix, Portland cement, sand, stone chips (≤10 mm) and water were used with a ratio of 1:1.49:2.51:0.5 by weight. The nominal strength of concrete cylinder was considered 25 MPa during the mix design. During concrete casting, three concrete cylinders were made from same concrete mixture. The nominal height and diameter of a cylinder was 300 mm and 150 mm. The concrete cylinders were cured in a water container for 28 days. The compressive tests of the cylinders were conducted according to the guideline of BS EN 12390-3 (2009) and the average strength value obtained is 26.1 MPa.

2.3 Test set-up and procedure

The four-point bending tests were performed to study the flexural response of CFAT and BAT beams. The gap between two end supports was 900 mm, while the gap between two loading points and shear span was 300 mm. A 600 kN capacity hydraulic machine was utilized for the tests. A displacement control load of 1.5 mm/min was applied during the tests. Roller supports were used to allow movement along longitudinal direction and rotation around bending axis of the specimens. Underneath the loading points steel plates were used to prevent concentration of stresses on the specimens. Furthermore, inside BAT beams wooden blocks were located at supports and loading points for distributing the loads. During the tests, three LVDTs were positioned at loading points and mid-span of the bottom flange of the specimens to measure the vertical displacement. To record longitudinal strain, two strain gauges were installed at upper and lower faces of the specimens. A data logger was used to record all data during the tests. Figure 2 presents a snapshot and a schematic drawing of the test set-up.

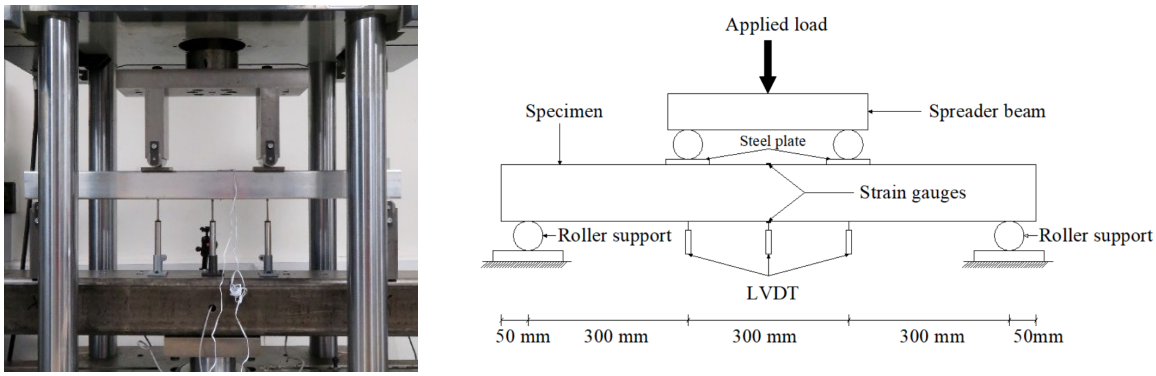

(a) Photograph (b) Schematic diagram

Figure 2. Test set-up and instrumentation.

3 TEST RESULTS

3.1 Failure modes

Figure 3 presents the typical modes of failure of the bare and concrete-filled specimens obtained from the tests. It is observed that all specimens failed by yielding (Figure 3(a)). Besides yielding, inward and outward local buckling were spotted between the loading points on the top flange and upper side of the web of most of the BAT specimens (Figure 3(b)). However, in CFAT specimens inward buckling was absent and outward buckling was comparatively smaller than the corresponding BAT specimens. This is related to the fact that the concrete infill prevented the forming of inward buckling and delayed the development of outward buckling. Moreover, some specimens (i.e., 101.6×50.8×3.3, 76.2×76.2×1.6-C, 76.2×76.2×3.3-C, 101.6×50.8×3.3-C and 101.6×76.2×3.3-C) experienced fracture at the tension side of the tube after reaching ultimate bending moment (Figure 3(c)). Table 3 summarises the failure modes of all specimens observed during the tests.

(a) 76.2×76.2×4.8-C (b) 76.2×76.2×4.8 (c) 6.2×76.2×3.3-C

Figure 3. Typical failure modes, (a) Yielding, (b) Local buckling, (c) Fracture in tension zone of tube.

Table 3. Modes of Failure of specimens.

Specimen	Failure mode	Specimen	Failure mode
76.2×76.2×1.6	LB	76.2×76.2×1.6-C	Y+LB+TF
76.2×76.2×3.3	LB	76.2×76.2×3.3-C	Y+LB+TF
76.2×76.2×4.8	Y+LB	76.2×76.2×4.8-C	Y+LB
76.2×76.2×6.4	Y+LB	76.2×76.2×6.4-C	Y
76.2×25.4×3.3	Y	76.2×25.4×3.3-C	Y
76.2×38.1×3.3	Y	76.2×38.1×3.3-C	Y
76.2×50.8×3.3	Y+LB	76.2×50.8×3.3-C	Y+LB
101.6×25.4×3.3	Y+LB	101.6×25.4×3.3-C	Y+ LB
101.6×50.8×3.3	Y+LB+TF	101.6×50.8×3.3-C	Y+LB+TF
101.6×76.2×3.3	LB	101.6×76.2×3.3-C	Y+LB+TF
Note: Y = Yielding, LB = Local buckling, TF = Tensile fracture			

3.2 Flexural strength

Using the experimental data, the bending moment versus mid-span deflection graphs of CFAT and BAT beams are plotted in Figure 4. The maximum bending moment obtained from the curve is considered as the flexural strength of the corresponding specimen and the values of all specimens are listed in Table 4. It can be observed from the figure and table that due to existence of concrete in the CFAT specimens, the flexural strength is significantly enhanced compared to the counterpart bare specimens. In Table 4, the percentage increase of flexural strength of CFAT specimens compared to BAT specimens is also presented. It is found that percentage increase is highest for 76.2×76.2×1.6-C which is 64.17% and for specimen 76.2×76.2×6.4-C the value is lowest which is 4.48%. This indicates that when the width and depth of a cross-section are constant, the strength improvement decreases with the increase of wall thickness. This is attributed to the inner concrete that slows down the formation of local buckling of slender cross-sections, thereby resulting in gaining additional strength. Moreover, it is also observed that when the thickness is constant, the percentage increase is higher for specimens with larger cross-sections. This is attributed to the larger cross-section which offers more confinement to the inner concrete, resulting in addition of extra strength.

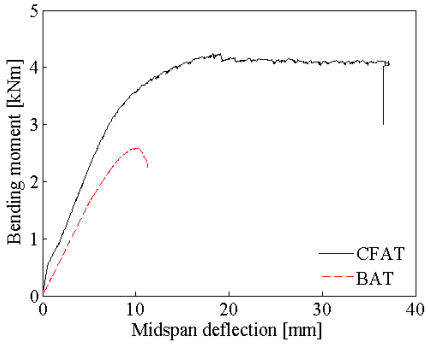

(a) 76.2×76.2×1.6 (-C)

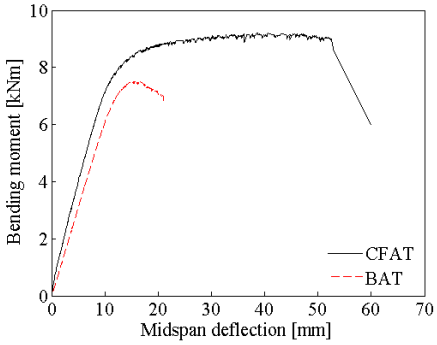

(b) 76.2×76.2×3.3 (-C)

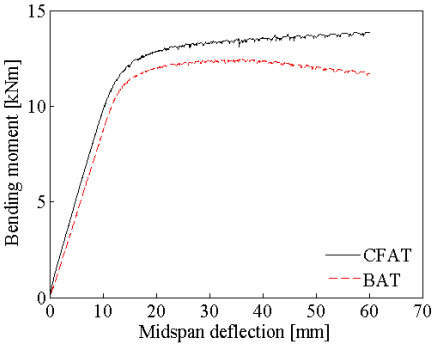

(c) 76.2×76.2×4.8 (-C)

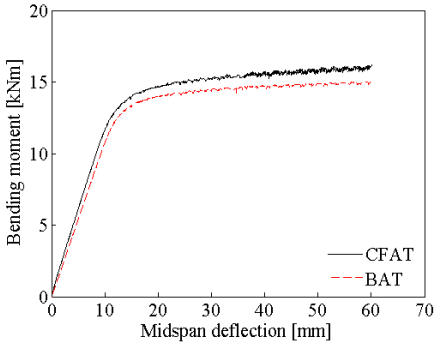

(d) 76.2×76.2×6.4 (-C)

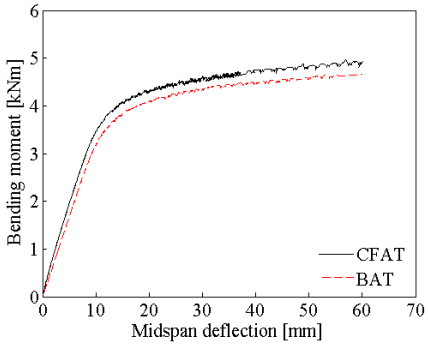

(e) 76.2×25.4×3.3 (-C)

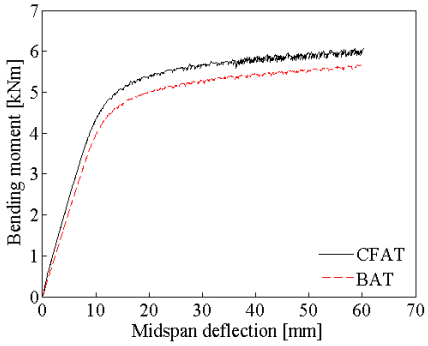

(f) 76.2×38.1×3.3 (-C)

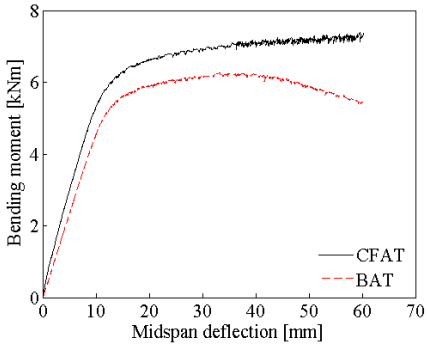

(g) 76.2×50.8×3.3 (-C)

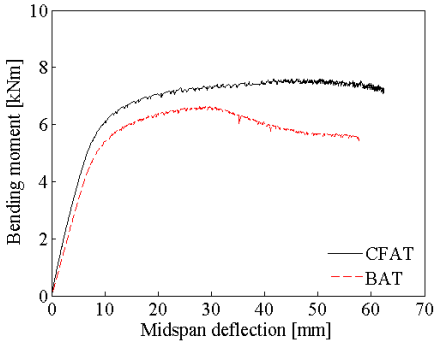

(h) 101.6×25.4×3.3 (-C)

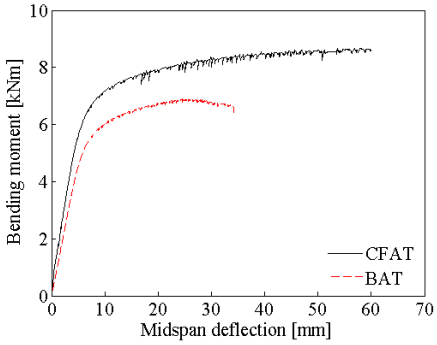

(i) 101.6×50.8×3.3 (-C)

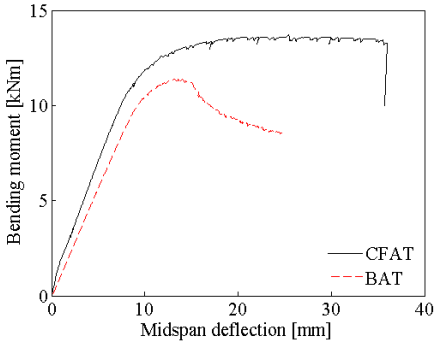

(j) 101.6×76.2×3.3 (-C)

Figure 4: Bending moment versus mid-span deflection graphs of specimens.

Table 4. Flexural strength of specimens.

Specimen	M_{BAT} (kNm)	Specimen	M_{CFAT} (kNm)	$(M_{CFAT} - M_{BAT}) / M_{BAT}$ (%)
76.2×76.2×1.6	2.59	76.2×76.2×1.6-C	4.25	64.17
76.2×76.2×3.3	7.52	76.2×76.2×3.3-C	9.01	19.84
76.2×76.2×4.8	12.47	76.2×76.2×4.8-C	13.39	7.37
76.2×76.2×6.4	14.54	76.2×76.2×6.4-C	15.33	5.43
76.2×25.4×3.3	4.46	76.2×25.4×3.3-C	4.60	3.14
76.2×38.1×3.3	5.38	76.2×38.1×3.3-C	5.66	5.20
76.2×50.8×3.3	6.27	76.2×50.8×3.3-C	6.93	10.56
101.6×25.4×3.3	6.64	101.6×25.4×3.3-C	7.25	9.18
101.6×50.8×3.3	6.84	101.6×50.8×3.3-C	8.31	21.52
101.6×76.2×3.3	11.39	101.6×76.2×3.3-C	13.73	20.54

3.3 Flexural stiffness and ductility

Based on the experimental data, the flexural stiffness and ductility of BAT and CFAT flexural members are calculated by Eq. (1) and (2), respectively and presented in Table 5.

$$K = \frac{0.2M_u L^2}{\pi^2 \delta} \tag{1}$$

$$\mu = \frac{\delta_u}{\delta_y} \tag{2}$$

where K is the flexural stiffness, μ is the ductility, M_u is flexural strength, δ is the mid-span vertical displacement at $0.2M_u$, δ_y is the mid-span vertical displacement at yield moment and δ_u is the mid-span vertical displacement at flexural strength.

It is observed from Table 5 that the flexural stiffness and the ductility of CFAT specimens are higher than that of BAT specimens. The improvement of stiffness is more pronounced for specimens with thinner sections.

4 DESIGN EQUATIONS FOR CFAT BEAMS

Due to absence of design standards for CFAT flexural members, in this study the design equations available for concrete-filled steel flexural members in Eurocode 4 (2004) are considered by substituting

the mechanical properties of steel with those of aluminium alloy. Based on Eurocode 4, the flexural capacity of CFAT beams can be determined by Eqs. (3).

$$M_{u,prop} = M_{pl} = \left(W_{pla} - W_{pla,n}\right) f_{0.2} + 0.5\left(W_{plc} - W_{plc,n}\right) f_c \tag{3}$$

In this equation, W_{pla} and W_{plc} are the plastic moduli of a hollow and concrete section, respectively, calculated by Eq. (4) and (5). $W_{pla,n}$ and $W_{pla,n}$ are the plastic moduli of a hollow and concrete section at $2h_n$, determined by Eq. (6) and (7). h_n is the distance between the centreline and the centroid of the composite section which is calculated by Eq. (8). In this equation, A_c and f_c are area and compressive strength of concrete, respectively.

$$W_{pla} = \frac{BH^2}{4} - \frac{2}{3}(t)^3 - (t)^2(4-\pi)\left(\frac{H}{2} - t\right) - W_{plc} \tag{4}$$

$$W_{plc} = \frac{(B-2t)(H-2t)^2}{4} \tag{5}$$

$$W_{pla,n} = Bh_n^2 - W_{plc,n} \tag{6}$$

$$W_{plc,n} = (B-2t)h_n^2 \tag{7}$$

$$h_n = \frac{A_c f_c}{2Bf_c + 4t(2f_{0.2} - f_c)} \tag{8}$$

Table 5. Flexural stiffness and ductility of the specimens.

Specimen	***K* (kNm²)**	**(K_{CFAT} - K_{BAT}) / K_{BAT} (%)**	**δ_y (mm)**	**δ_u (mm)**	**μ**	**(μ_{CFAT}-μ_{BAT}) / μ_{BAT} (%)**
76.2×76.2×1.6	29.95	55.63	4.72	10.10	2.14	48.66
76.2×76.2×1.6-C	46.61		5.80	18.45	3.18	
76.2×76.2×3.3	51.85	40.60	7.32	15.92	2.17	205.44
76.2×76.2×3.3-C	72.90		6.89	45.77	6.64	
76.2×76.2×4.8	72.50	23.79	8.60	37.53	4.36	64.39
76.2×76.2×4.8-C	89.75		8.37	60.02	7.17	
76.2×76.2×6.4	90.02	16.25	8.36	59.98	7.17	3.04
76.2×76.2×6.4-C	104.65		8.12	60.03	7.39	
76.2×25.4×3.3	28.23	22.14	8.47	60.01	7.09	4.30
76.2×25.4×3.3-C	34.48		8.13	60.08	7.39	
76.2×38.1×3.3	34.21	23.71	8.29	60.01	7.24	4.95
76.2×38.1×3.3-C	42.32		7.90	60.02	7.60	
76.2×50.8×3.3	36.87	45.49	8.14	41.67	5.12	57.25
76.2×50.8×3.3-C	53.64		7.48	60.24	8.05	
101.6×25.4×3.3	55.17	35.94	6.07	30.22	4.98	57.83
101.6×25.4×3.3-C	75.00		5.90	46.36	7.86	
101.6×50.8×3.3	77.61	47.39	4.49	27.30	6.08	120.31
101.6×50.8×3.3-C	114.39		4.48	60.01	13.40	
101.6×76.2×3.3	91.21	44.56	6.05	13.63	2.25	163.40
101.6×76.2×3.3-C	131.85		5.91	35.07	5.93	

The design flexural strengths of all CFAT specimens predicted using Eq. (3) are listed in Table 6 and compared with flexural strengths obtained from the experiments. The mean value of the tset over the proposed moment ratio ($M_u/M_{u,prop}$) is 1.04, indicating that the proposed design equations provide good prediction of the flexural capacity of CFAT beams.

Table 6. Comparison of experimental flexural strength with design flexural strength.

Specimen	M_u	$M_{u,prop}$	$M_u/M_{u,prop}$
76.2×76.2×1.6-C	4.49	4.25	0.95
76.2×76.2×3.3-C	8.84	9.01	1.02
76.2×76.2×4.8-C	12.49	13.87	1.11
76.2×76.2×6.4-C	14.88	16.18	1.09
76.2×25.4×3.3-C	4.69	4.97	1.06
76.2×38.1×3.3-C	5.72	6.07	1.06
76.2×50.8×3.3-C	6.59	7.38	1.12
101.6×25.4×3.3-C	7.49	7.60	1.01
101.6×50.8×3.3-C	9.21	8.68	0.94
101.6×76.2×3.3-C	13.38	13.73	1.03
		Mean	1.04
		COV	0.06

5 CONLUSIONS

This paper presented an experimental study on the behaviour of square and rectangular CFAT and BAT beams under in-plane bending. Total 20 beams were tested, including 10 CFAT and 10 BAT specimens. Based on the observed results the following points can be concluded:

1) The flexural strength, flexural stiffness and ductility of CFAT specimens are significantly enhanced up to 64.17%, 55.63% and 205.44%, respectively compared to the counterpart BAT specimens. This indicates that the concrete infill effectively reduced the formation and extentension of local buckling of BAT specimens.
2) It is demonstrated that the increase of flexural strength due to concrete infill was prominent for thinner sections. This is attributed to the inner concrete that slows down the formation of local buckling of slender cross-sections, thereby resulting in gaining additional strength.
3) Due to the absence of design standards for CFAT beams, in this study the design equations available for concrete-filled steel tubular flexural members in the Eurocode 4 are considered by substituting the mechanical properties of steel with those of aluminium alloy. The mean and COV values of the ratio of experimental and design flexural strength are found 1.04 and 0.06, respectively. It is indicated that the proposed design equations provide good predictions of flexural capacity of CFAT beams.

6 ACKNOWLEDGEMENTS

The authors are thankful for the help of the staffs of the Schools of Civil Engineering and Built Environment and Engineering at Liverpool John Moores University. The authors would like to acknowledge the financial support of the Faculty of Engineering and Technology of Liverpool John Moores University.

REFERENCES

BS EN ISO 6892-1. (2009). *Metallic Materials – Tensile Testing – Part 1: Method of test at room temperature*. European Committee for Standardization (CEN), Brussels.

BS EN 12390-3. (2009). *Testing hardened concrete. Compressive strength of test specimens*. European Committee for Standardization, Brussels.

Chen, Y., Feng, R. & Wang, L. (2017a). Flexural behaviour of concrete-filled stainless steel SHS and RHS tubes. *Engineering Structures, 134*, 159–171.

Chen, Y., Wang, K., Feng, R., He, K. & Wang, L. (2017b). Flexural behaviour of concrete-filled stainless steel CHS subjected to static loading. *Journal of Constructional Steel Research, 139*, 30–43.

Eurocode 4 (EC4), BS EN 1994-1-1. (2004). *Eurocode 4: Design of Composite Steel and Concrete Structures. Part 1-1: General Rules and Rules for Buildings*. European Committee for Standardisation.

Feng, R., Sun, W., Shen, C. & Zhu, J. (2017). Experimental investigation of aluminum square and rectangular beams with circular perforations. *Engineering Structures*, *151*, 613–632.

Georgantzia, E., Gkantou, M. & Kamaris, G. S. (2021). Aluminium alloys as structural material: A review of research. *Engineering Structures, 227:111372*.

Han, L. H. (2004). Flexural behaviour of concrete-filled steel tubes. *Journal of Constructional Steel Research, 60(1–2)*, 313–337.

Hou, C. C., Han, L. H., Wang, Q. L. & Hou, C. (2016). Flexural behavior of circular concrete filled steel tubes (CFST) under sustained load and chloride corrosion. *Thin-Walled Structures,107*, 182–96.

Kissell, J. & Ferry, R. (2002). Aluminum structures: a guide to their specifications and design. *New York John Wiley Sons*.

Lu, Y. Q. & Kennedy, D. J. L. (1994). The flexural behaviour of concrete-filled hollow structural sections. *Canadian Journal of Civil Engineering, 21(1)*, 111–130.

Mazzolani, F. M. (2004). Competing issues for aluminium alloys in structural engineering. *Progress in Structural Engineering and Materials, 6(4),* 185–196.

Mazzolani, F. M. (1995). *Aluminium alloy structures (2nd ed.)*. London Chapman Hall.

Montuori, R. & Piluso, V. (2015). Analysis and modeling of CFT members: moment curvature analysis. *Thin-Walled Structures, 86(1)*, 157–166.

Moen, L. A., Langseth, M. & Hopperstad, O. S. (1999a). Rotational capacity of aluminium beams under moment gradient I: experiments. *Journal of the Structural Division (ASCE), 125(8)*, 910–920.

Moen, L. A., Hopperstad, O. S. & Langseth, M. (1999b). Rotational capacity of aluminium beams under moment gradient II: numerical simulations. *Journal of the Structural Division (ASCE), 125(8)*, 921–929.

Patel, V., Liang, Q. & Hadi, M. (2020). Numerical simulations of circular high strength concrete-filled aluminum tubular short columns incorporating new concrete confinement model. *Thin-Walled Structures,* 147:106492.

Su, M., Young, B. & Gardner, L. (2014). Deformation-based design of aluminium alloy beams. *Engineering Structures*, 80, 339–349.

Zhang, T., Gong, Y., Ding, F., Liu, X. & Yu, Z. (2021). Experimental and numerical investigation on the flexural behavior of concrete-filled elliptical steel tube (CFET). *Journal of Building Engineering*, 41:102412.

Zhu, J. H. & Young, B. (2008). Behavior and design of aluminum alloy structural members. *Advanced Steel Construction, 4*, 158–172.

Zhu, J. H. & Young, B. (2009). Design of Aluminum Alloy Flexural Members Using Direct Strength Method. *Journal of the Structural Division (ASCE), 135(5)*, 558–566.